Journal of Alloys and Compounds, 195 (1993) 93–96
JALCOM 7422

Microstructures and Precipitates in Laser-Ablated YBCO Thin Films on $SrTiO_3$ (110)

A. Catana[a] and C. Rossel

IBM Research Division, Zurich Research Laboratory, 8803 Rüschlikon, Switzerland

A. Perrin, M. Guilloux-Viry and C. Thivet

Laboratoire de Chimie du Solide et Inorganique Moléculaire, U.R.A. C.N.R.S. 1495, Université de Rennes I, Avenue Général Leclerc, F-35042 Rennes Cédex, France

[a]Now at Prospectives et Recherche, EPFL, 1015 Lausanne, Switzerland

Abstract

Thin YBCO films (~ 100 nm) have been deposited by laser ablation on $SrTiO_3$ (110) substrates. Microstructural investigations have been performed by scanning tunneling and high-resolution electron microscopy. The results show that the surface corrugation is related to the growth of twisted YBCO domains that nucleate at the film/substrate interface. The twist is characterized by a 90° rotation of YBCO around the [100] and/or [010] axes, which results in {013} and/or {103} planes parallel to the substrate surface. Precipitates belonging to Y_2O_3 are densely distributed on the film surface. No such second phases have been identified inside the YBCO films. The orientational relationship between precipitates and film is such that the lattice mismatch is minimized in the interface planes. A large number of precipitates grow from the film surface outwards. This phenomenon can be explained on the basis of lattice matching arguments and favorable growth kinetics.

1. Introduction

The microstructure and composition of thin superconducting YBCO films have been the subject of a large number of studies. In particular, considerable effort has recently been devoted to the investigation of second phases present inside and on the surface of YBCO films as obtained by a variety of techniques on $SrTiO_3$ (100) substrates [1-4]. Although several studies have addressed the question of YBCO grown on $SrTiO_3$ (110) [5,6], little is known about the occurrence of second phases in such films. Knowledge about second phases in nonstoichiometric YBCO films on $SrTiO_3$ should contribute to a more general understanding of phase diagrams and growth processes. In particular it is interesting to clarify the relationship between the growth of second phases and the film morphology in the case of YBCO/$SrTiO_3$ (110). Such correlations have been suggested for growths on $SrTiO_3$ (100) [1,2,7-9].

In this contribution we investigate the microstructure of superconducting YBCO films grown by laser ablation on $SrTiO_3$ (110) substrates. Combining scanning tunneling (STM) and transmission electron (TEM) microscopy, we correlate the surface topology with characteristic structural features of the film. In particular, high-resolution electron microscopy (HREM) and electron diffraction are used to identify second-phase precipitates as epitaxial Y_2O_3. Their epitaxial orientations and growth will be discussed on the basis of lattice matching arguments and compared to recent results.

2. Experimental

Thin YBCO films have been grown by laser ablation with an excimer laser operating at 308 nm under an oxygen pressure of 0.3-0.5 mbar. Typical substrate temperatures were between 720 and 750 °C.

The films were structurally characterized by X-ray diffraction (θ -2θ scans, rocking curves, Weissenberg camera in oscillating crystal mode), electron channeling patterns and *in-situ* reflection high energy electron diffraction. The difference between (103) and (110) oriented YBCO films could be unambiguously assessed. Details are given in Ref. 10. The superconducting properties of the films were studied by ac susceptibility and four probe resistance measurements. The (103) films show a sharp superconducting transition with $T_c(R=0)$ between 85 and 89 K.

The STM is a beetle-like model operating in air. Pt-Ir tips are used. Typical tunneling currents are $I \leq 1$ nA at bias tip voltages of $V \leq -0.8$ V [11].

0925-8388/93/$06.00

1993 – Elsevier Sequoia

TEM samples were prepared for cross-sectional investigations by standard mechanical thinning and polishing techniques as well as ion milling with effective liquid nitrogen cooling. The observations were performed on a Jeol JEM-2010 operating at 200 kV.

3. Results and Discussion

3.1. Film structure

An STM micrograph of the surface of YBCO (103) film grown on $SrTiO_3$ (110) is displayed in Fig. 1. The corrugation is described by elongated plateaus along the [001] substrate axis with typical widths of 10-100 nm and heights of about 15-20 nm. The surface roughness characterizing the growth on $SrTiO_3$ (110) is correlated with the structure of the film. Indeed, HREM investigations (Fig. 2) show that YBCO grows with two orientations related by a 90° twist around the [010] axis: (a) (103) YBCO ‖ (110) $SrTiO_3$, (010) YBCO ‖ (001) $SrTiO_3$; (b) ($\bar{1}$03) YBCO ‖ (110) $SrTiO_3$, (010) YBCO ‖ (001) $SrTiO_3$ (see also [5,7,8]). These situations are schematically represented in the inset of Fig. 2. Note however that two other orientational relationships have to be considered: (a') (013) YBCO ‖ (110) $SrTiO_3$, (100) YBCO ‖ (001) $SrTiO_3$; (b') (0$\bar{1}$3) YBCO ‖ (110) YBCO, (100) YBCO ‖ (001) $SrTiO_3$. These couples correspond to twists around the [100] YBCO axis. Since these latter couples are not distinguishable from the (a,b) relations, we will refer to a single pair of twist orientations in the following.

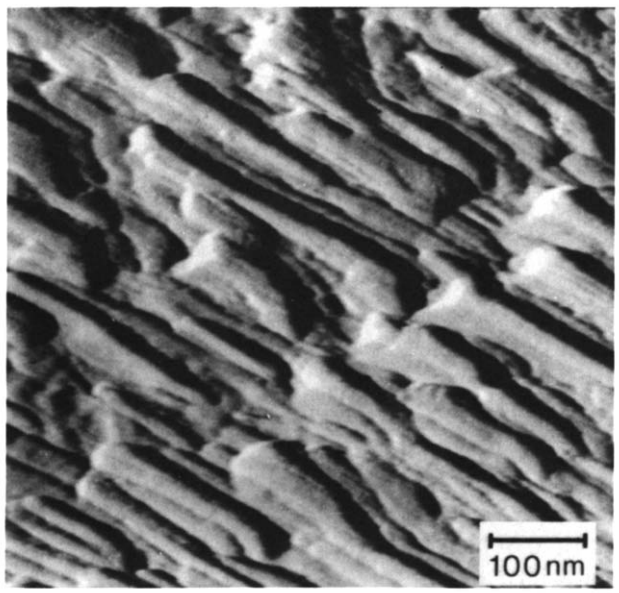

Figure 1. STM image of a YBCO (103) film on $SrTiO_3$ (110). Tunneling parameters: $V = -0.8$ V, $I = 0.3$ nA.

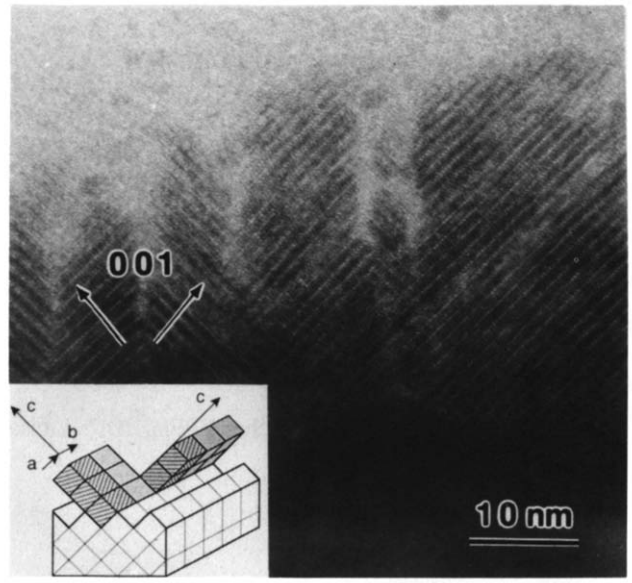

Figure 2. HREM cross-sectional view of the twisted YBCO film shown in Fig. 1. Inset: Schematic of (103) and ($\bar{1}$03) growth orientations on $SrTiO_3$ (110).

The twisted YBCO domains with typical widths between 3 and 30 nm are generated at the substrate surface and grow through the entire film thickness. Sporadically, twisted grains nucleate within the film as indicated by an arrow in Fig. 2. This can be explained by the occurrence of unstable regions created by the joining of growth fronts propagating from different nucleation sites on the substrate surface. The HREM results confirm the observations made by scanning electron microscopy on a larger scale and are certainly representative of the entire film. A more detailed study of the surface topology and microstructure of (103) and (110) films will be published elsewhere [11].

3.2. Precipitates

The dark-field micrograph in Fig. 3a shows that second phases (bright regions) lie on the film surface. Electron diffraction (Fig. 3b) identifies the particles as cubic Y_2O_3 ($a = 1.06$ nm) growing such that <110> Y_2O_3 ‖ <100> YBCO and {100} Y_2O_3 ‖ {001} YBCO. Owing to the twisted YBCO (001) surfaces, Y_2O_3 grows with two orientations related by a 90° rotation around its <110> axis.

These epitaxial relationships minimize the lattice mismatch in the interface planes. Indeed, the *a,b*-plane of YBCO has the smallest lattice mismatch to {100} Y_2O_3: 3% along <110> Y_2O_3 ‖ <100> YBCO, with a nearly coincident cell area of 1.1 nm^2.

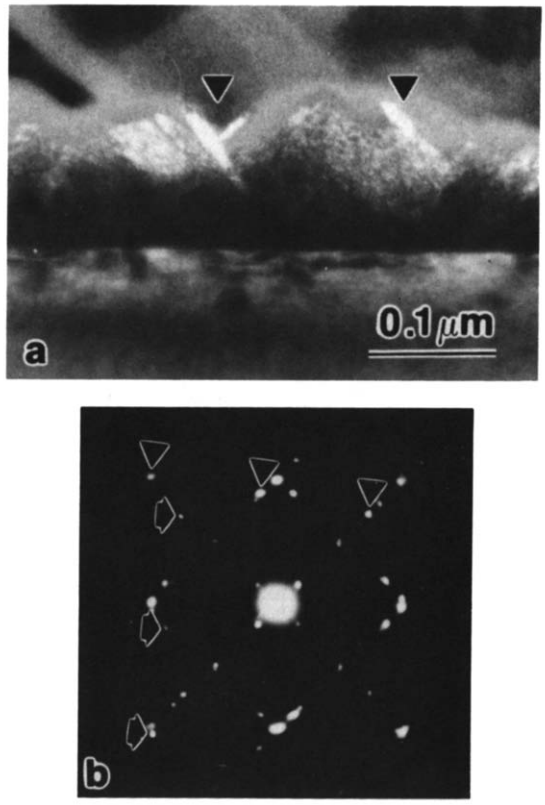

Figure 3. (a) Dark-field TEM cross-sectional view ($g = 220_{SrTiO_3}$) showing the presence of Y_2O_3 outgrowths (arrows). (b) Electron diffraction pattern along <110> Y_2O_3 || <100> YBCO. Two sets of arrows indicate the two Y_2O_3 orientations rotated by 90°

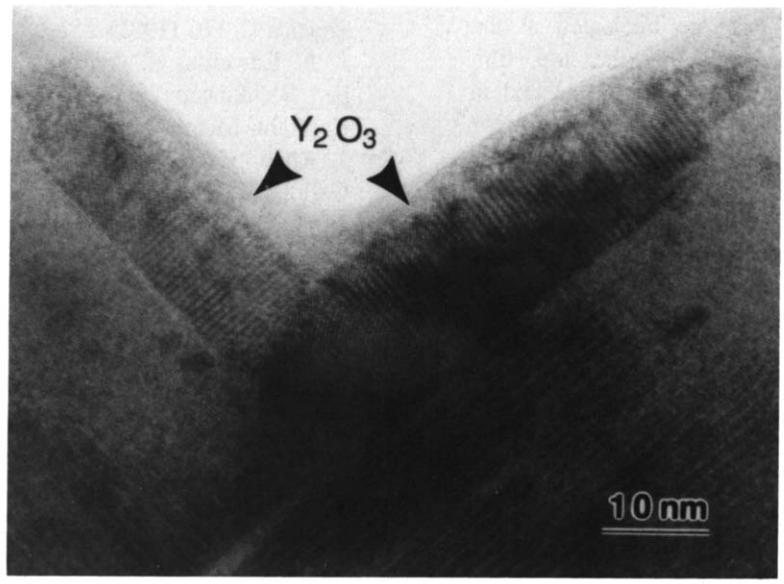

Figure 4. HREM cross-sectional view of two Y_2O_3 particles lying on twisted YBCO (100) surfaces (arrows).

The precipitates are characterized by a tabular shape with long planar {100} facets parallel to the YBCO (001) planes (Fig. 4), which are probably due to the favorable matching conditions of the interfacial planes. The high growth rate of the precipitates along the YBCO (001) planes favors outgrowths as observed in Fig. 3.

Y_2O_3 precipitates with the orientational relationship described above have already been observed in sputtered [1] and chemical vapor-deposition grown [4] films on $SrTiO_3$ (100). However, in those cases the precipitates are present both inside the films as well as on their surface. This discrepancy may well be related to the different structure of the YBCO films. Indeed, the formation of twists in the case of growth on $SrTiO_3$ (110) creates a large number of domain boundaries not present in films on $SrTiO_3$ (100). These boundaries are favorable paths for the diffusion of trapped atoms through the film to the top surface, where favorable nucleation conditions stabilize the precipitate structure. As such, segregation of second phases on the surface may be a general feature of twisted YBCO films deposited on $SrTiO_3$ (110).

4. Conclusion

STM and HREM were combined to investigate the surface topology and microstructure of thin YBCO (103) films grown on $SrTiO_3$ (110). The results show that the surface corrugation is related to the growth of twisted YBCO domains. These are nucleated at the film/substrate interface and grow to the top film surface, thereby creating elongated plateaus stacked in a toothlike structure. The twists are described by 90° rotations along the [010] and/or [100] YBCO axes, bringing {103} and/or {013} planes parallel to $SrTiO_3$ (110).

Precipitates with well-defined tabular shapes have been identified as Y_2O_3. They grow on the YBCO (001) surface facets with an epitaxial orientation that minimizes the lattice mismatch: <110> Y_2O_3 || <100> YBCO and {100} Y_2O_3 || {001} YBCO. In some cases these precipitates are extending out of the YBCO surface, suggesting that Y_2O_3 is characterized by faster growth rates than YBCO. The observation that Y_2O_3 lie exclusively on the film surface, as opposed to previous reports relating to films deposited on $SrTiO_3$ (100), suggests that grain boundaries are favorable diffusion paths for excess material. Such boundaries are densely distributed in films grown on $SrTiO_3$ (110).

Acknowledgments

The authors gratefully acknowledge R.F. Broom for his valuable support, as well as the financial support of the Swiss National Science Foundation.

References

1 A. Catana, R. F. Broom, J. G. Bednorz, J. Mannhart and D. G. Schlom, Appl. Phys. Lett. 60 (1992) 1016, and references therein.
2 T. I. Selinder, U. Helmersson, Z. Han, J.-E. Sundgren, H. Sjöström and L. R. Wallenberg, to appear in Physica C.
3 H. Yamane, K. Takagi, T. Oku, E. Aoyagi, K. Hiraga, K. Wanatabe, N.Kobayashi and T. Hirai, Int'l Workshop on Superconductivity, Honolulu, 1992.
4 P. Lu, Y. Q. Li, J. Zhao, C. S. Chern, B. Gallois, P. Norris, B. Kear and F. Cosandey, Appl. Phys. Lett. 60 (1992) 1265.
5 T. Terashima, Y. Bando, K. Iijima, K. Yamamoto and K. Hirata, Appl. Phys. Lett. 53 (1988) 2232.
6 S. Takeno, S. Nakamura, M. Sagoi and T. Miura, Physica C 176 (1991) 151.
7 J. A. Edwards, N. G. Chew, S. W. Goodyear, S. E. Blenkinsop and R.G.Humphries, J. Less Common Metals 164 (1990) 414.
8 J. Zhao, C. S. Chern, Y. Q. Li, P. Norris, B. Gallois, B. Kear, X.D. Wu and R.E. Münchhausen, Appl. Phys. Lett. 58 (1991) 2839.
9 R. Ramesh, A. Inam, D. M. Hwang, T. D. Sands, C. C. Chang and D. L. Hart, Appl. Phys. Lett. 58 (1991) 1557.
10 M. Guilloux-Viry, A. Perrin, C. Thivet, M. Sergent, C. Rossel and A. Catana, submitted to J. Cryst. Growth.
11 C. Rossel, A. Catana, A. Perrin, M. Guilloux-Viry and C. Thivet, to be published.